The fracture of a rubber-modified epoxy polymer containing through-thickness and surface cracks

G. Davy, S. Hashemi and A.J. Kinloch

(Imperial College of Science, Technology and Medicine, London, UK)

The critical stress-intensity factor, K_{Ic}, for crack initiation has been determined using many different test geometries for a rubber-toughened epoxy polymer. A main difference between the test geometries is that some employ a through-thickness crack whilst others contain an embedded surface crack. A detailed study of the applicability of linear-elastic fracture-mechanics (LEFM) has been conducted and, when only valid LEFM results are considered, it has been shown that the values of K_{Ic} are independent of test geometry. Thus, the results from a through-thickness crack are the same as those obtained from a surface crack. Further, the particular aspect of slow crack growth on the determination of K_{Ic} is considered in detail.

Key words: crack growth; failure mechanisms; fractography; fracture mechanics; linear-elastic fracture mechanics; plastic-zone size; rubber toughened epoxy

A linear-elastic fracture-mechanics (LEFM) approach to the characterization of the failure of adhesives and adhesive joints is very commonly adopted[1-5]. LEFM has been used, for example, to investigate the problem of environmental attack upon adhesive joints, to study the dynamic and static fatigue fracture of joints and to investigate the mechanisms of toughening of multiphase rubber-modified epoxy adhesives.

The basis of LEFM is that a characteristic parameter may be defined which describes the toughness or crack resistance of the adhesive or the adhesive joint. The parameters typically determined are the plane-strain Mode I (tensile-opening mode) values of the fracture energy, G_{Ic}, or the critical stress-intensity factor, K_{Ic}; these two parameters may be related via the modulus of the adhesive[4]. The value of G_{Ic} or K_{Ic} should, within certain well established limits, be independent of the details of the test geometry or loading conditions employed. However, it has been suggested that the toughness of an adhesive, as assessed by determining the plane-strain values of G_{Ic} or K_{Ic}, may be different if the specimen geometry contains an embedded crack, as opposed to a through-thickness crack; the latter type of crack usually being used to determine the values of G_{Ic} or K_{Ic}. The reasoning behind the suggestion is that an embedded crack, such as a surface crack or a circular penny-shaped crack, is surrounded to a greater extent by elastic material, which might restrict the amount of crack tip plasticity which develops, and hence result in a lower toughness being measured, even though the through-thickness test geometries are designed to ensure plane-strain conditions are present. One source of this suggestion has been the work conducted[6,7] using a 'blister' test geometry, where the crack is totally embedded in the adhesive or joint. However, in this specimen only relatively blunt initial cracks can be inserted in a typical, high modulus, epoxy adhesive. This prevents valid measurements of the fracture energy, G_{Ic}, or the critical stress-intensity factor, K_{Ic}, being obtained.

The importance of this suggestion is that if the values of K_{Ic}, for example, are significantly lower for the case of an embedded crack, then this must be taken into account when using K_{Ic} values for design or life-prediction studies. The work described in the present paper was conducted in order to resolve the issue of whether a LEFM approach to determining the values of the critical stress-intensity factor, K_{Ic}, for crack initiation in a rubber-modified epoxy polymer, typical of the current generation of structural adhesives, would yield truly geometry-independent values of K_{Ic}. Of special interest was to establish whether the values of K_{Ic} are dependent upon whether a through-thickness or an embedded surface crack is employed.

0413-7496/89/020069-08 $03.00

Table 1. Formulation of the rubber-modified epoxy adhesive

Ingredient	Rubber-modified epoxy (phr*)
DGEBA epoxy resin	100
Piperidine	5
CTBN rubber	15

*phr = parts per hundred of resin

Experimental

Materials

The epoxy polymer examined in the present study was a model material based upon a rubber-toughened epoxy resin. The epoxy resin employed was derived from the reaction of bisphenol A and epichlorohydrin and was largely composed of the diglycidyl ether of bisphenol A (DGEBA). The curing agent was piperidine. The rubber used to prepare the multiphase, rubber-modified epoxy adhesive material was a carboxyl-terminated, random copolymer of butadiene and acrylonitrile (CTBN rubber: carboxyl content 2.37 wt %, molecular weight 3500 g mol^{-1}). The formulation of the rubber-modified epoxy resin is shown in Table 1.

To prepare sheets of the rubber-modified epoxy the CTBN rubber was added to the epoxy resin and hand-mixed for approximately 5 to 10 min. This mixture was heated to 65 ± 5°C in a water bath and mixed for 5 min using an electric stirrer and then degassed in a vacuum oven at 60°C until frothing stopped. When the mixture had cooled to below 30°C the piperidine was mixed in gently to minimize air entrapment. The rubber-epoxy mixture was poured into a preheated mould, cured at 120°C for 16 h and allowed to cool slowly. The formulation and cure schedule described results in the rubber-modified material having a two-phase microstructure with a volume fraction of rubbery particles of 0.18 with an average particle size of 1.6 μm[8]. The glass transition temperature of the epoxy is 100 ± 2°C.

Preparation of test specimens

The specimens were prepared by first casting sheets of the rubber-toughened epoxy polymer, as described above, which were 9.78 mm in thickness and then machining the sheets to the dimensions shown in Figs. 1 and 2. Sharp cracks were inserted by carefully machining a notch of radius approximately 12 μm into the sheets as indicated in Figs 1 and 2. Cracks of various depths, a, were made using this technique. Previous work has shown that for these relatively tough polymers this method of crack insertion results in a crack tip of sufficient sharpness to give true minimum values of the critical stress-intensity factor, K_{Ic}[9].

Testing of specimens

The specimens were tested at a temperature of 20°C using a screw-driven tensile-testing machine, which was operated in displacement control at a rate of 2 mm min^{-1}. The load, P, versus displacement, δ, trace was obtained for each test. After the test had been completed the fracture surfaces were examined, the depth, a, of the original crack was measured and the mean value from (typically) six readings ascertained. This mean value of crack length was used to determine the value of the stress-intensity factor. For the through-thickness specimens four to six replicates were examined for each particular geometry and for each crack length employed.

Analysis of data

The critical stress-intensity factor, K_{Ic}, for crack initiation is given by

$$K_{Ic} = \sigma_c Y a^{1/2} \quad (1)$$

where $\sigma_c$is the applied stress at crack initiation, Y is the geometry factor and a is the crack depth at the onset of crack growth. The value of the geometry factor, Y, is usually a function of the ratio of the crack length to another dimension of the specimen. Thus, to ascertain the value of K_{Ic} for any particular specimen geometry the appropriate value of Y needs to be determined.

Compact tension (CT) geometry

The compact tension specimen is shown in Fig. 1(a) and contains a through-thickness crack. It is a standard test geometry and the value of the critical applied stress, σ_c, is given by

$$\sigma_c = P_c/BW \quad (2)$$

where P_c is the applied load, B is the thickness and W is the width of the specimen, as defined in Fig. 1(a). The value of the geometry factor, Y, is given by[10]

$$Y = \left(\frac{W}{a}\right)^{1/2} \frac{(2 + a/W)}{(1 - a/W)^{3/2}} [0.886 + 4.64(a/W) - 13.32(a/W)^2 + 14.72(a/W)^3 - 5.6(a/W)^4] \quad (3)$$

Single-edge notch bend (SENB) geometry

The SENB specimen contains a through-thickness crack and is shown in Fig. 1(b). The values of the critical applied stress, σ, and the geometry factor, Y, are given by[10]

$$\sigma_c = 3P_cS/2BW^2 = 6P_c/BW \quad (4)$$

for $S/W = 4$ and

$$Y = 1.93 - 3.07(a/W) + 14.53(a/W)^2 - 25.11(a/W)^3 + 25.80(a/W)^4 \quad (5)$$

where S is the span and is defined, with the other geometric parameters, in Fig. 1(b).

Single-edge notch tension (SENT) geometry

The SENT specimen contains a through-thickness crack and is shown in Fig. 1(c). The values of the critical applied stress, σ_c, and the geometry factor, Y, are given by Equation (2) and[11]

$$Y = 1.99 - 0.41(a/W) + 18.70(a/W)^2 - 38.48(a/W)^3 + 53.85(a/W)^4 \quad (6)$$

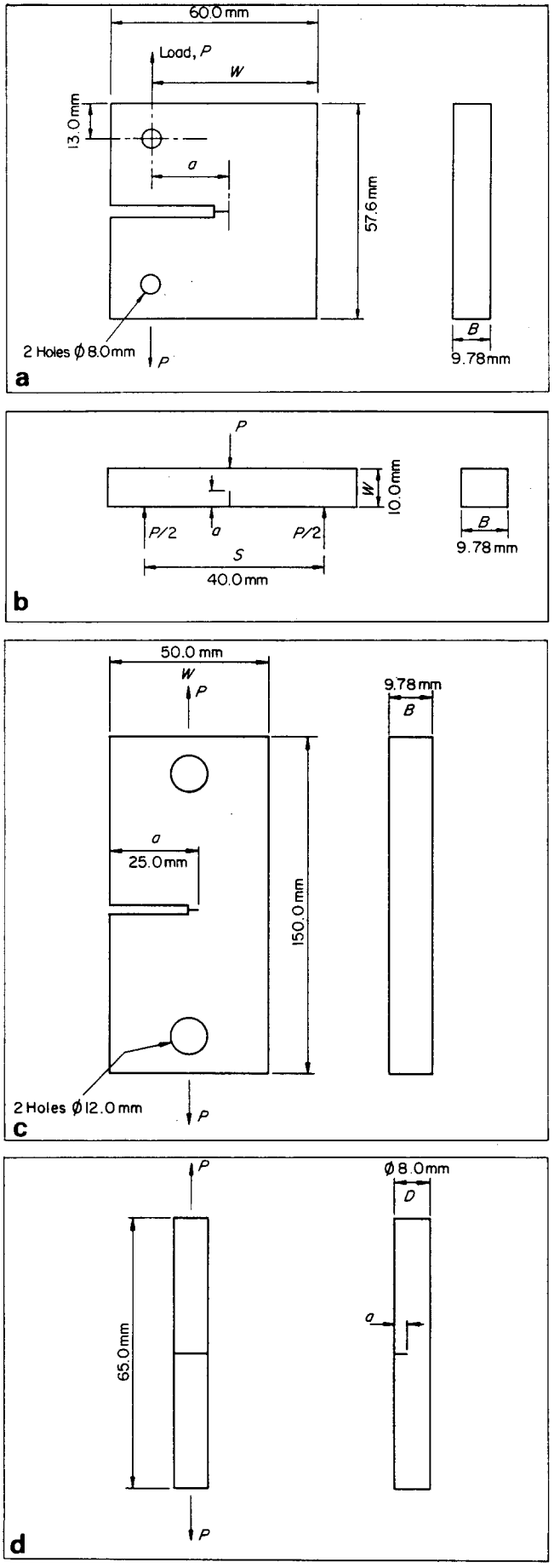

Fig. 1 Specimens containing through-thickness cracks: (a) compact tension (CT) specimen, (b) single-edge notched bend (SENB) specimen, (c) single-edge notch tension (SENT) specimen, and (d) edge-notch in circular bar in tension (ENCB) specimen

Edge-notch in circular bar in tension (ENCB) geometry

The ENCB specimen contains a through-thickness crack and is shown in Fig. 1(d). The values of the critical applied stress, σ_c, and the geometry factor, Y, are given by[12]

$$\sigma_c = 4P_c/\pi D^2 \tag{7}$$

and

$$Y = \pi^{1/2}[1.11 - 3.59(a/D) + 24.87(a/D)^2 - 53.39(a/D)^3 + 57.23(a/D)^4] \tag{8}$$

for $0.063 < a/D < 0.563$ where D is the diameter of the bar, as defined in Fig. 1(d).

Surface-notch bend (SNB) geometry

The SNB specimen contains an embedded surface crack and is shown in Fig. 2(a). The values of the critical applied stress, σ_c, and the geometry factor, Y, are given by Equation (4) and[13, 14]

$$Y = \frac{Q_{fs}[1 + 0.12(1 - a/2c)^2]\,[1 - 1.36(a/W)(a/c)^{0.1}]}{[(1 + 1.47(a/c)^{1.64}]^{0.5}}\,\pi^{1/2} \tag{9}$$

where $2c$ is the length of the circular surface crack, a is the depth of the crack, see Fig. 2(a), and Q_{fs} is a further geometry correction factor for the finite width of the specimen. The value of Q_{fs} is given by[15]

$$Q_{fs} = 1 + \frac{FGH}{(0.2745)^2} \tag{10}$$

where

$$F = 0.381 - 0.141(a/c) - 0.366(a/c)^2 + 0.569(a/c)^3 - 0.248(a/c)^4 \tag{11}$$

$$G = -0.0239 + 1.434(c/B) - 2.984(c/B)^2 + 7.822(c/B)^3 \tag{12}$$

$$H = -0.0113 + 0.323(a/W) + 0.749(a/W)^2 - 0.535(a/W)^3 \tag{13}$$

for a/c, $2c/B$ and $a/W < 0.5$.

Surface-notch tension (SNT) geometry

The SNT specimen contains an embedded surface crack and is shown in Fig. 2(b). The values of the critical applied stress, σ_c, and the geometry factor, Y, are given by Equation (2) and[16, 17]

$$Y = \frac{\pi^{1/2}\,1.2^{1/2}}{[1 + 1.464(a/c)^{1.65}]^{0.5}} \tag{14}$$

for $a/c \leqslant 1$. This value of Y includes a finite specimen correction and the terms a and c are defined in Fig. 2(b).

Results and discussion

Applicability of LEFM

To obtain a valid measurement of the critical stress-intensity factor, K_{Ic}, several criteria have to be met. Essentially, the effects of the specimen thickness, B, the specimen width, W, and the degree of non-linearity of the load *versus* deflection trace must all be considered.

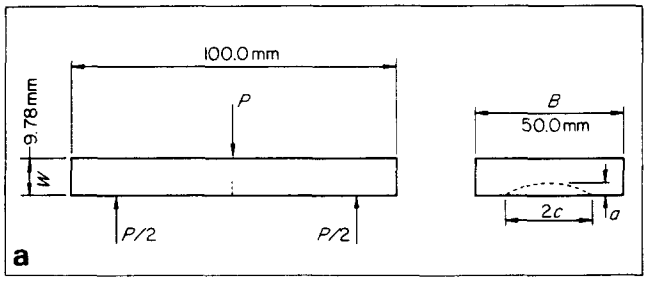

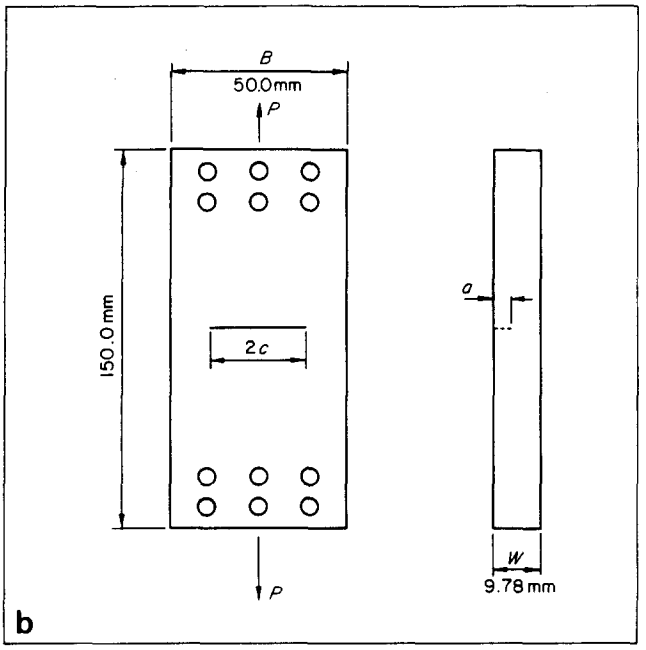

Fig. 2 Specimens containing surface cracks: (a) surface-notch bend (SNB) specimen, and (b) surface-notch tension (SNT) specimen

The effect of the thickness, B, of the specimen arises because the state of stress near the crack tip varies from plane stress in the surface regions of a relatively thick specimen, or throughout the thickness of a thin plate, to plane strain in the centre of a thick plate. Now the stress at which a material yields is greater in a triaxial stress field (plane strain) than in a biaxial stress field (plane stress): in the former more constrained case a less extensive degree of plasticity develops at the crack tip, and a lower toughness is observed. Hence, the thickness, B, of the specimen must be sufficient to ensure that the state of stress throughout most of the specimen is plane strain. Such a stress state results in the minimum value of the critical stress-intensity factor, K_{Ic}, being measured[10, 18, 19]. The minimum thickness, B_{min}, needed for plane-strain conditions to dominate is usually taken to be

$$B_{min} \geqslant 2.5\,(K_Q/\sigma_y)^2 \qquad (15)$$

where K_Q is the provisional value of the critical stress-intensity factor, but whose validity is not yet established, and σ_y is the uniaxial yield stress of the material. The value of σ_y for the rubber-toughened epoxy, equivalent to the rate of test used for the fracture mechanics measurements, was taken to be 57 MPa[20]. For all the fracture-mechanics specimens the value of the minimum thickness, B_{min}, needed was between 4 and 6 mm and, since B was always about 10 mm or greater, the condition that $B > B_{min}$ was easily fulfilled.

A second condition for a valid LEFM test is that

$$W_{min} \geqslant 5\,(K_Q/\sigma_y)^2 \qquad (16)$$

where W_{min} is the minimum width of the specimen which is needed. This arises from the need to avoid excessive plasticity in the ligament $(W - a)$. If the stress in the ligament approaches the yield stress then the value of critical stress-intensity factor that is determined will be underestimated. The value of W_{min} was typically between 6 and 12 mm, depending upon the exact specimen geometry, and in all cases the specimen width, W, that was used was chosen such that the condition $W > W_{min}$ was fulfilled.

The third requirement that has to be met is that the load, P, *versus* displacement, δ, trace is essentially linear. The trace may be non-linear for a variety of reasons; *eg* due to excessive plasticity occurring at the crack tip, due to inelastic or plastic deformations occurring in the bulk of the specimen or due to slow crack growth prior to the maximum load being attained. The latter example will obviously also give rise to problems in defining the exact value of the load, P_c, for crack initiation. Since, if slow crack growth occurs before the maximum load is attained, a value of the critical stress-intensity factor for crack initiation based upon the maximum load will be an overestimate of the toughness of the material. These problems may be overcome, at least to a good approximation, by following the arbitrary rule embodied in the ASTM standard for testing metals[18]. A load *versus* displacement diagram is shown in Fig. 3 and a best straight line is drawn to determine the compliance, C; the value of C is given by δ/P. This is then increased

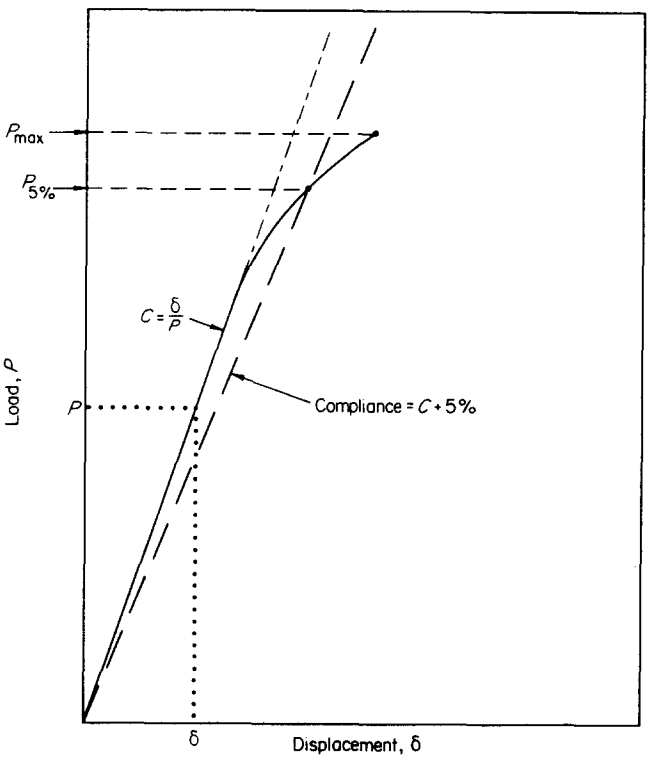

Fig. 3 A load *versus* displacement trace showing how P_{max} and $P_{5\%}$ are determined

by 5% and a further line drawn for this new value of compliance, *ie* $C + 5\%$. (Increasing the compliance by 5% is equivalent to allowing for a certain percentage of crack growth; for example it is equivalent to approximately a 2.5% increase in crack length in the case of a single-edge notched bend test specimen.) Now, if the $C + 5\%$ line intersects the load curve then $P_{5\%}$ is found and this is taken as the load at crack initiation.

Further, for the value of K_Q based upon either the value of P_{max} or $P_{5\%}$ to be valid then the following criteria must be met:

$$P_{max}/P_{5\%} < 1.1 \quad (17)$$

This condition essentially allows 10% non-linearity of the load *versus* displacement trace before the experimental measurements are declared to be too non-linear for LEFM to apply. Thus, to summarize, if $P_{max}/P_{5\%} > 1.1$ then the test is invalid. If $P_{max}/P_{5\%} < 1.1$ then $P_{5\%}$ is used in the calculation of K_Q, or alternatively P_{max}, if the value of P_{max} falls within the two lines. For the present tests the load versus displacement trace often exhibited a degree of non-linearity, apparently due to slow crack growth occurring prior to the maximum load being attained. However, the condition that $P_{max}/P_{5\%} < 1.1$ was always met, except for the edge-notch circular-bar (ENCB) tests.

Through-thickness crack specimens

The four geometries which were used to assess the critical stress-intensity factor, K_Q, for the specimens containing the through-thickness cracks were the compact tension (CT), the single-edge notch tension (SENT), the single-edge notch bend (SENB) and edge-notch circular-bar (ENCB) specimens, see Fig. 1. The results are shown in Table 2.

Several interesting observations may be made from the data shown in Table 2. The results for the ENCB specimen do meet the criterion that $P_{max}/P_{5\%} < 1.1$, *ie* the non-linearity of the load *versus* displacement trace for the specimen is too great for LEFM to be applicable and any value of the stress-intensity factor determined from these tests will be invalid. The reason is probably due to the detailed geometry of this specimen. A small increase in crack length results in a relatively large fractional increase in cracked area, and hence a relatively large increase in the compliance of the cracked specimen. However, all the conditions for the applicability of LEFM are met for the three remaining test geometries. Some slow crack growth was observed in the CT and SENB geometries, hence values for $K_Q(5\%)$ and for $K_Q(max)$ are quoted, where the former value was calculated using $P_{5\%}$ and the latter using P_{max}. It was seen that, within experimental error, the load corresponding to crack initiation, as measured directly by using a travelling microscope, is very similar in value to that given by the value of $P_{5\%}$. Finally, for the valid LEFM tests the coefficients of variation associated with the values of K_Q were between $\pm 7\%$ and $\pm 12\%$ and, from using a 'student's *t*-test' statistical method, it is found that there is no significant dependence of the value of K_Q upon either the a/W ratio in the case of the CT specimen or the actual specimen geometry employed. Both observations are in agreement with the basic principles of using a LEFM approach which attempts to define a characteristic fracture parameter.

Surface-crack specimens

The two geometries which were used to assess the critical stress-intensity factor, K_Q, for the specimens containing the surface cracks were the surface-notch bend (SNB) and the surface-notch tension (SNT) specimens, see Fig. 2. The results are shown in Table 3.

As may be seen, the results from the SNB and SNT tests were all valid, with no indication of any non-linearity of the associated load *versus* displacement traces. Hence, only values of $K_Q(max)$ may be deduced. Again there appears to be no dependence of the value of K_Q upon either the a/W ratio in the case of the SNB specimen or the actual specimen geometry employed; both observations in agreement with the basic principles of using a LEFM approach.

Comparison of results

The values of the critical stress-intensity factor for crack initiation, K_{Ic}, from the specimens containing either through-thickness or surface cracks are shown in Table 4. In this table only results from tests where valid LEFM conditions were found to apply have been used to calculate the mean and standard deviation for the K_{Ic} values. Also, for the specimens containing

Table 2. Values of the critical stress-intensity factor, K_Q, for the specimens containing the through-thickness cracks

Specimen	a/W ratio	$K_Q(5\%)$ (MPa $m^{1/2}$)	$K_Q(max)$ (MPa $m^{1/2}$)
Compact tension (CT)	0.45	2.55	2.58
	0.47	2.83	2.87
	0.49	2.40	2.44
	0.50	2.71	2.72
Single-edge notch bend (SENB)	0.51	2.25	2.29
Single-edge notch tension (SENT)	0.50	*	2.45
Edge-notch circular bar (ENCB); a/D =	0.21	1.24	2.19
	0.29	1.11	2.14

*For the edge-notch circular-bar tests $P_{max}/P_{5\%} > 1.1$; hence the test is invalid.

Table 3. Values of the critical stress-intensity factor, K_Q, for the specimens containing the surface cracks

Specimen	a/W ratio	$K_Q(5\%)$ (MPa $m^{1/2}$)	$K_Q(max)$ (MPa $m^{1/2}$)
Specimen-notch bend (SNB)	0.21	-	2.71
	0.26	-	2.34
	0.31	-	2.60
	0.42	-	2.66
	0.43		2.66
Surface-notch tension (SNT)	0.41	-	2.50

Table 4. Comparison of the values of the critical stress-intensity factor, K_{Ic}, for crack initiation from specimens containing through-thickness or surface cracks

Specimen type	K_{Ic} (MPa $m^{1/2}$)
Through-thickness cracks	2.55 ± 0.21
Surface cracks	2.58 ± 0.14

through-thickness cracks, the values of $K_Q(5\%)$ were used for the CT and SENB specimens and the value of $K_Q(max)$ for the SENT specimen.

As may be seen from the results shown in Table 4, there is no significant difference in the values of K_{Ic} from the two different types of specimens used. Thus, providing the criteria for applying LEFM are followed, the value of K_{Ic} determined from using an embedded crack is no different to that from using a through-thickness crack. An overall value of K_{Ic} of 2.56 ± 0.17 MPa $m^{1/2}$ may be calculated from the results given in Tables 2 and 3. This value is in excellent agreement with a previously quoted[20,21] value of 2.39 MPa $m^{1/2}$, which was ascertained at the same rate of test from solely using the CT specimen.

Fractography

Examination of the fracture surfaces from the various specimens clearly confirmed the observations made whilst conducting the fracture tests and when analysing the load *versus* displacement traces. For example, photographs of the fracture surfaces from a CT specimen (having a through-thickness crack) and a SNB specimen (having a surface crack) are shown in Figs 4 and 5, respectively. In both figures the position of the initial crack may be seen, and immediately ahead of the initial crack a stress-whitened region is visible. This stress-whitened region is associated with the deformation processes that occur at the crack tip in the rubber-toughened epoxy. These deformation processes involve both cavitation in the rubber, and multiple, but localized, shear yielding in the matrix initiated by the stress concentrations induced by the rubbery particles[2,21]. It is the cavitated particles which give rise to the stress whitening effect seen in Figs 4 and 5. This effect is indicative of the development of a relatively large plastic zone at the crack tip and/or slow crack growth in the material where the slowly growing crack has a relatively large plastic zone at its tip. Ahead of the white zone is a matt region which arises from the crack growth becoming unstable, and the crack propagating relatively fast through the specimen. The fast moving crack has a far higher local strain rate at its tip, hence the local yield stress is higher and the extent of plastic shear deformation at the crack tip is far lower. Indeed, the differences in the appearance of the fracture surface in the stress-whitened region and the fast-fracture regions are also clearly evident in the scanning electron micrographs shown in Fig. 6. The presence of more extensive cavitation in the rubber particles and more extensive plasticity in the matrix is readily observable in the fracture surface corresponding to the white-zone region.

Now the extent of the plastic zone ahead of the initial crack may be deduced from[19]

$$r_y = (1/6\pi)\ (K_{Ic}/\sigma_y)^2 \qquad (18)$$

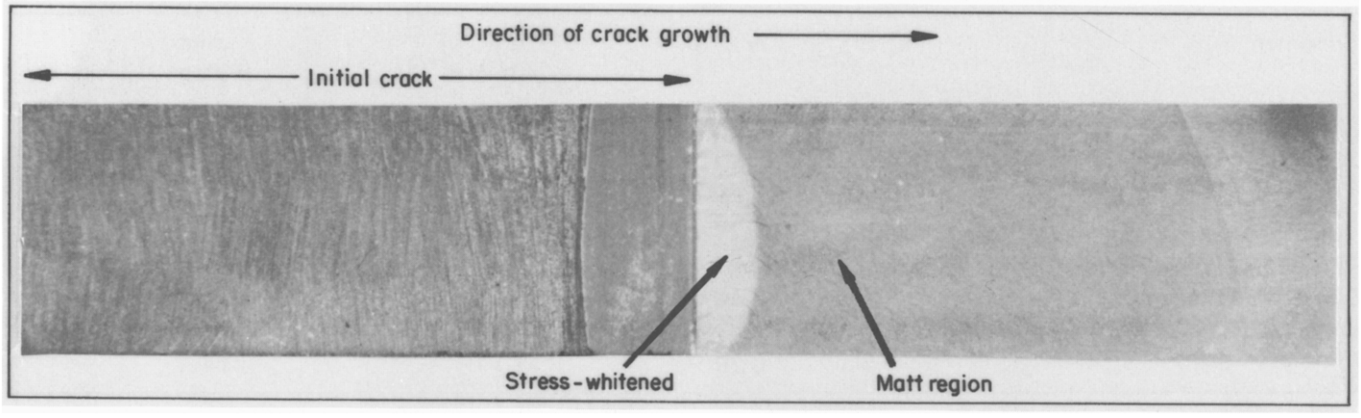

Fig. 4 The fracture surface from a CT specimen (containing a through-thickness crack)

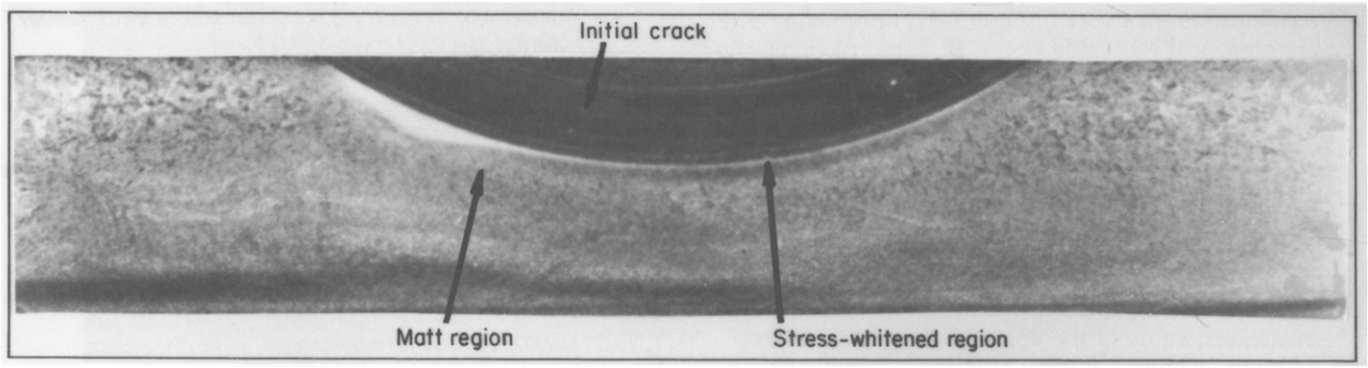

Fig. 5 The fracture surface from a SNB specimen (containing a surface crack).

where r_y is the radius of the plastic zone. Hence, since the values of K_{Ic} and σ_y are 2.54 MPa $m^{1/2}$ and 57 MPa respectively, the value of the calculated length of the plastic zone, $2r_y$, is about 0.2 mm. From Fig. 5, the length of the stress-whitened zone ahead of the crack in the SNB specimen is estimated to be generally 0.2 to 0.3 mm, and from scanning electron micrographs of this region, *eg* Fig. 7, is estimated to be about 0.2 to 0.25 mm. Thus, the conclusion is that the stress-whitened region ahead of the initial crack in the SNB specimen is solely associated with the development of the plastic zone ahead of the crack; when the crack starts to grow it does so rapidly through the plastic zone which has formed and then through the rest of the specimen. This mode of crack growth is in agreement with the observations from the load *versus* displacement trace, where no indication of any slow crack growth was recorded. In contrast, the photograph (Fig. 4) of the *CT* specimen shows a large stress-whitened region which is now associated with the development of the plastic zone at the crack tip and slow crack growth in the material, where the slowly growing crack has a relatively large plastic zone at its tip. The size of the initial plastic zone that develops ahead of the initial crack would be the same as that for the SNB specimen, but this parameter cannot be estimated from Fig. 4. This is because the crack has slowly propagated, with a large plastic zone at its tip, for some distance before the crack has become unstable and propagated rapidly through the specimen. It is not possible to distinguish which portion of the white region seen on the fracture surface is associated with the initial development of the plastic zone and which portion is associated with the subsequent slow crack growth. The slow crack growth causes the corresponding load *versus* displacement trace to be non-linear and the value of the stress-intensity factor for initiation has to be deduced by using a travelling microscope to observe directly the crack initiating in

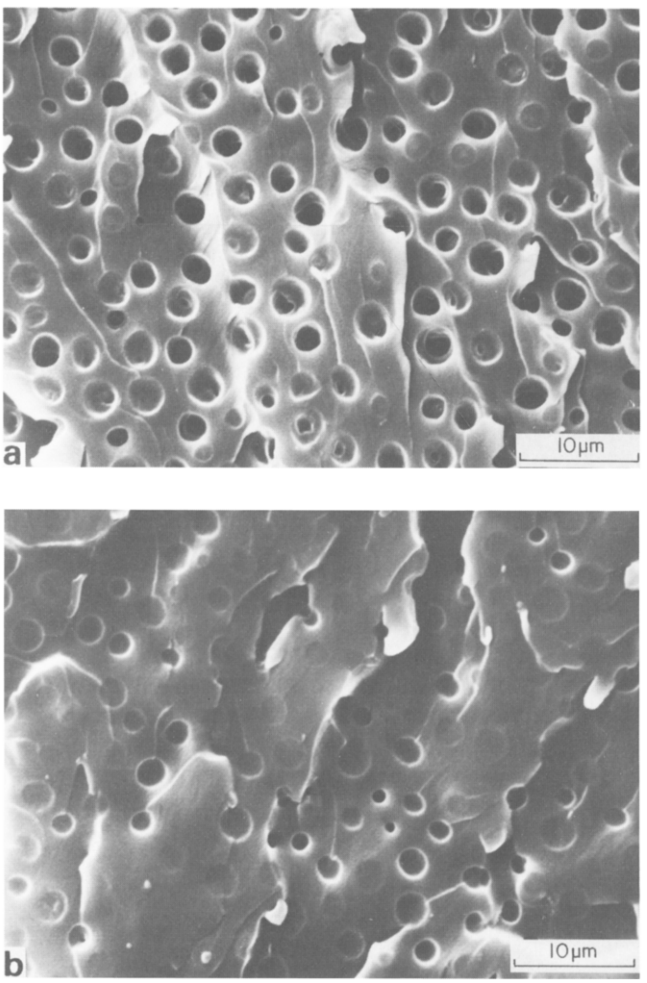

Fig. 6 Typical scanning electron micrographs of the fracture surfaces: (a) from the stress-whitened region (note the extensive cavitation of the rubber particles and the extensive plastic deformation of the epoxy matrix), and (b) from the matt region where fast crack propagation has occurred

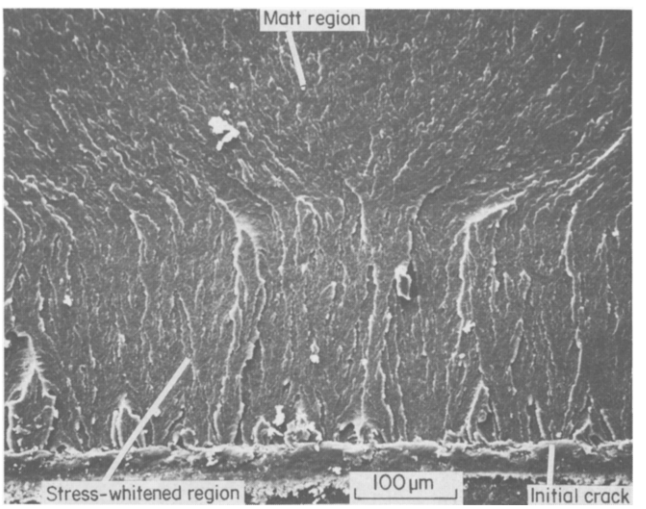

Fig. 7 Scanning electron micrograph of the fracture surface from a SNB specimen showing the stress-whitened region between the initial crack and the matt region.

the *CT* specimen, a very difficult task, or by using the more empirical $P_{5\%}$ value.

Conclusions

The critical stress-intensity factor, K_{Ic}, for crack initiation has been determined from many differest test geometries for a rubber-toughened epoxy polymer. A main difference between the test geometries is that some employ a through-thickness crack whilst others contain an embedded surface crack.

A detailed study of the applicability of LEFM has been conducted and, when only valid LEFM results are considered, values of K_{Ic} are independent of test geometry. Thus, the results from using a through-thickness crack are the same as those from using an embedded surface crack.

Of particular interest has been the problem of the crack initiating with a relatively slow velocity, which is typically associated with the crack initiating at a load below the maximum recorded load. By using the standard fracture-mechanics techniques an offset load has been taken as the appropriate value of the load to use in calculating the value of K_{Ic}. This approach has been supported both from direct observations on the crack initiation process and from examining the resulting fracture surfaces.

Acknowledgements

A.J. Kinloch would like to acknowledge the University of Utah, College of Engineering, for a Visiting Professorship, during which the present paper was prepared.

References

1 **Mostovoy, S. and Ripling, E.** *J Appl Polym Sci* **10** (1966) p 1351

2 **Bascom, W.D. and Cottington, R.L.** *J Adhesion* **7** (1976) p 333

3 **Kinloch, A.J. and Shaw, S.J.** *J Adhesion* **12** (1981) p 59

4 **Kinloch, A.J.** *'Adhesion and Adhesives: Science and Technology'* (Chapman and Hall, London, 1987) p 264

5 **Anderson, G.P. and DeVries, K.L.** *J Adhesion* **23** (1987) p 289

6 **Andrews, E.H. and Stevenson, A.** *J Mater Sci* **13** (1978) p 1680

7 **Parry, T.V. and Wronski, A.S.** *'Adhesion 5'* ed K.W. Allen (Applied Science Publishers, London, 1981) p 1

8 **Kinloch, A.J. and Hunston, D.L.** *J Mater Sci Lett* **6** (1987) p 137

9 **Kinloch, A.J. and Kodokian, G.K.A.** *J Adhesion* **24** (1987) p 109

10 *'A LEFM standard for determining* K_c *and* G_c *for plastics'* (European Fracture Group, 1987)

11 **Brown, W.F. and Srawley, J.E.** *ASTM STP 410* (1966) p 12

12 **Daoud, O.E.K. and Cartwright, D.J.** *Engng Fracture Mech* **19** (1984) p 701

13 **Koterazawa, R. and Minamisaka, S.** *J Soc Mater Sci Japan* **26** (1977) p 1

14 **Smith, F.W., Emery, A.F. and Kobayashi, A.S.** *J Appl Mechs Trans ASME* **89** (1967) p 953

15 **Holbrook, S.J. and Dover, W.D.** *Engng Fract Mech* **12** (1979) p 347

16 **Newman, J.C.** *ASTM STP 687* (1979) p 16

17 **Irwin, G.R.** *J Appl Mech* **29** (1962) p 651

18 *Standard E-399* (American Society for Testing and Materials 1978)

19 **Kinloch, A.J. and Young, R.J.** *'Fracture Behaviour of Polymers'* (Applied Science Publishers, London, 1983) p 74

20 **Kinloch, A.J., Shaw, S.J. and Hunston, D.L.** *Polymer* **24** (1983) p 1355

21 **Kinloch, A.J., Shaw, S.J., Tod, D.A. and Hunston, D.L.** *Polymer* **24** (1983) p 1341

Authors

The authors are with the Department of Mechanical Engineering, Imperial College of Science, Technology and Medicine, Exhibition Rd, London, SW7 2BX, UK. Enquiries should be addressed to A.J. Kinloch.